Photodissociation pathways of gas-phase photoactive yellow protein chromophores

Lutz Lammich, Jyoti Rajput, and Lars H. Andersen*
Department of Physics and Astronomy, University of Aarhus, 8000 Aarhus C, Denmark
(Received 23 July 2008; published 18 November 2008)

The absorption dynamics of two model chromophores of the photoactive yellow protein were studied in gas-phase experiments. Using different time-resolving techniques with an overall sensitivity ranging from seconds down to a few nanoseconds, complex dynamics were revealed for the *p*-coumaric acid anion, involving both fragmentation and electron detachment as possible photoresponse channels. For the *trans*-thiophenyl-*p*-coumarate model, despite its more complex molecular structure, simpler decay dynamics showing only fragmentation were observed.

DOI: 10.1103/PhysRevE.78.051916 PACS number(s): 87.15.mk, 33.20.Kf, 82.37.Vb

I. INTRODUCTION

Gas-phase studies of chromophore molecules have proven to be an important step toward a detailed understanding of photoactive proteins [1–6]. In contrast to liquid-phase experiments, the intrinsic properties of the chromophores can here be disentangled from environmental effects, which are known to have a major impact on both the absorption process and the following response of the molecule [7,8].

Being the functional centers of photoactive proteins, chromophores are found in a wide range of organisms and furthermore have many applications as markers in microbiological research [9]. In this work, we report on studies of the photoactive yellow protein (PYP) found in *Halorhodospira halophila* bacteria, which is one of the benchmark systems studied to gain insight into the mechanisms governing the photoresponse of light-sensitive proteins.

While the absorption spectrum of the PYP chromophore *in vacuo* has been studied earlier [10], we here focus on the *dynamics* of the photoinduced processes. To this end, the photofragmentation of two PYP model chromophores was studied on time scales ranging from milliseconds down to a few nanoseconds. The studied species are deprotonated *trans-p*-coumaric acid [pCA^-, Fig. 1(a)] and deprotonated *trans*-thiophenyl-*p*-coumarate [pCT^-; Fig. 1(b)], which have absorption maxima at 430 and 460 nm, respectively. The full absorption spectra can be found in [10].

It should be noted that the pCA^- chromophore ion has an isomer which is deprotonated at the phenol rather than the carboxyl group. In the technique applied here, the deprotonation takes place in the liquid phase, where the geometry depicted in Fig. 1(a) is the most stable one. However, it is not clear *a priori* if the deprotonation site is retained during the electrospray process [11]. Thus it cannot be excluded at this point that the phenolate form of PYP is present in our experiment. A more detailed investigation of this topic will be given in a separate presentation [12].

II. EXPERIMENTAL SETUP

To gain access to the dissociation dynamics of chromophore ions on nanosecond to millisecond time scales, two different experimental setups were used: a merged-beam apparatus employing an electrostatic storage ring sensitive on the microsecond to second time scale and a single-pass, crossed-beam setup covering the range from a few nanoseconds to about 2 μs. In both setups, electrospray-ion sources [13] are employed for producing a beam of negative (deprotonated) chromophore ions. The chromophore molecules are first dissolved in methanol, and small charged droplets of this solution are then formed by electrospray ionization. The solvent is evaporated in a heated capillary and the remaining ions are collected in a radio frequency ion trap using helium as a buffer gas.

At the repetition rate of the experiment, few-μs-long bunches of ions are extracted from the trap and accelerated to beam energies around 20 keV. Finally, ions not having the desired charge-to-mass ratio are removed from the beam in a magnetic dipole field.

A. Merged-beam setup at the electrostatic ion storage ring, Aarhus

The electrostatic ion storage ring, Aarhus (ELISA) [14] was used for observing fragmentation dynamics on microsecond to millisecond time scales (see Fig. 2). The bunches of chromophore ions produced in the electrospray ion source are injected after mass selection into the storage ring, where they circulate for up to seconds at a beam energy of 22 keV. In a straight section of the ring, the ions are overlapped with

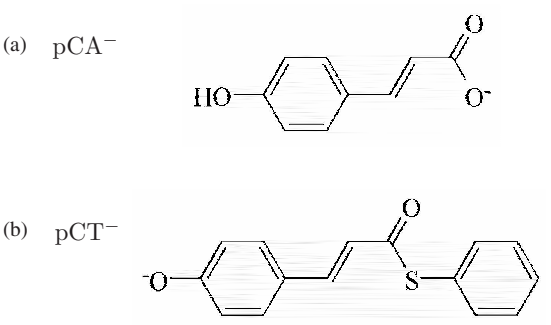

FIG. 1. Structure of the two model chromophores used in the present study: (a) deprotonated *trans-p*-coumaric acid (pCA^-); (b) deprotonated *trans*-thiophenyl-*p*-coumarate (pCT^-).

*lha@phys.au.dk

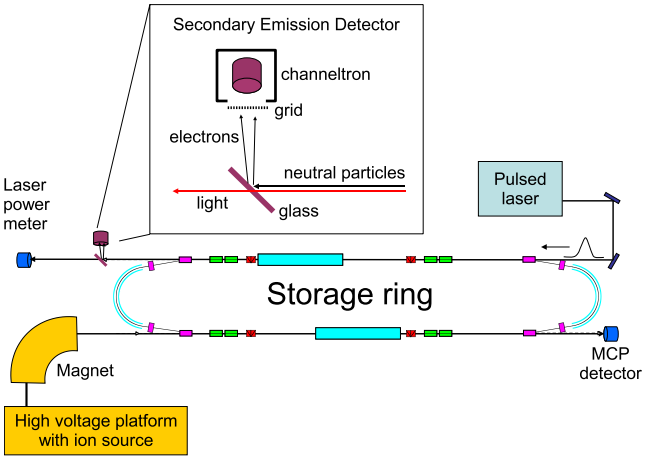

FIG. 2. (Color online) Ion storage ring ELISA with secondary emission detector.

a nanosecond laser pulse. Neutral fragments produced through photoabsorption (or by residual gas collisions) are recorded by two particle detectors located after both straight sections of the ring. For the ions studied here the revolution time in the ring is around 60 μs; thus a time resolution of 30 μs is reached when the data from both detectors are combined.

While a standard microchannel plate (MCP) detector is used in the section following the injection beamline, special care has to be taken when a detector is placed in the laser interaction section. Here neutral fragments travel parallel to the laser light. Since the latter needs to reach a power meter outside the vacuum chamber, a detector placed in this section has to register neutral particles while letting the laser light pass.

These requirements are met by a recently installed secondary emission detector (SED). By this technique [15], a glass plate is placed into the path of the laser light and the neutral particles. The glass is transparent for the laser wavelengths used here, but particles will be stopped and create secondary electrons. These are finally accelerated toward and registered by a standard channeltron detector. To avoid charging of the glass plate and to allow for the application of an accelerating voltage, the plate has a conductive coating (tin-doped indium oxide, In_2O_3:Sn). Note that the new detector arrangement not only increases the time resolution of photo-fragmentation studies at ELISA, but, most importantly, also allows for dead-time free detection of fragments produced immediately after photoabsorption.

Another new type of measurement recently realized at ELISA is the determination of the mass of daughter ions produced by fragmentation processes in the storage ring [16]. Here, the voltages of the ring's ion optics are switched shortly after the laser pulse such that closed ion orbits are reached for fragments with a certain fraction of the original molecule's mass. These daughter ions are kept in the ring for several revolutions and then registered on the MCP detector by switching off the deflection electrodes in front of this detector. The current setup is sensitive to daughter ions with a mass in the range 20–80 % of the parent ions at a resolution of a few percent.

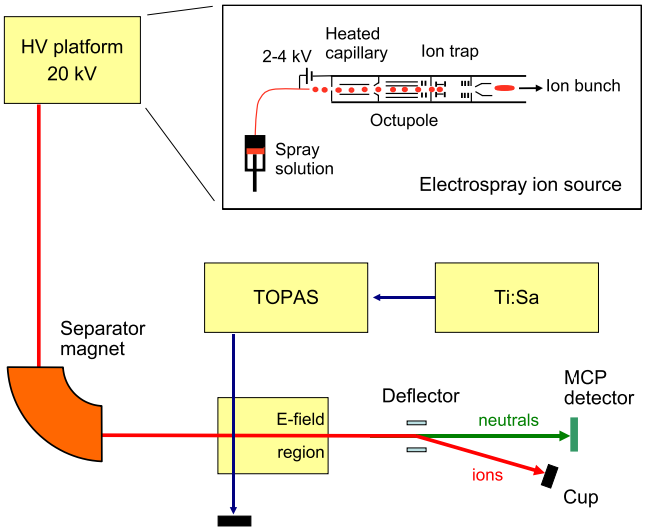

FIG. 3. (Color online) Overview of the single-pass ion beam and laser setup.

B. Single-pass, crossed-beam setup

To study the first microseconds of the decay process at higher time resolution, a crossed-beam setup is used, as depicted in Fig. 3. After production of the ions in an electrospray ion source, acceleration to 20 keV, and mass selection, the ion beam is here transported to an interaction region where it can be crossed with laser pulses of variable intensity and wavelength. The extraction from the ion trap (rate 2 kHz) and the firing of the laser are synchronized such that every second ion bunch is hit by a laser pulse. Those bunches that are not exposed to laser light are used to determine the number of background dissociations in the residual gas.

After the interaction region an electrostatic deflector separates the ion beam from neutral fragments, which are again produced either as a result of the photoabsorption process under study or due to residual gas collisions. The neutrals are registered by a MCP detector.

The laser pulses are produced by a Ti:sapphire femtosecond laser (wavelength 800 nm, pulse duration 120 fs, pulse energy ~0.8 mJ, repetition rate 1 kHz). To reach a wavelength within the absorption spectrum of the chromophore ions, the laser light is then either frequency doubled in a β-barium borate crystal or fed into an optical parametric amplifier (type TOPAS, Light Conversion Ltd.), which can deliver output wavelengths between 230 and 2900 nm.

For determining the dissociation times of the chromophore ions, that is, the time between the absorption of a photon and the emission of a neutral fragment, a velocity-tagging technique was used, as described in detail in [17]. In short, the ion beam is slowed down a few centimeters before the interaction point and then reaccelerated over a distance of ~20 cm in a homogeneous electric field (see Fig. 4). Neutral fragments that are formed during this reacceleration phase will not be affected by the electrical field, and thus continue their way to the detector at a reduced velocity, corresponding to the velocity of the parent ions at the time of the fragmentation. This reduced velocity manifests itself in an increased time of flight (TOF) of the neutral fragments from the laser interaction point to the MCP detector.

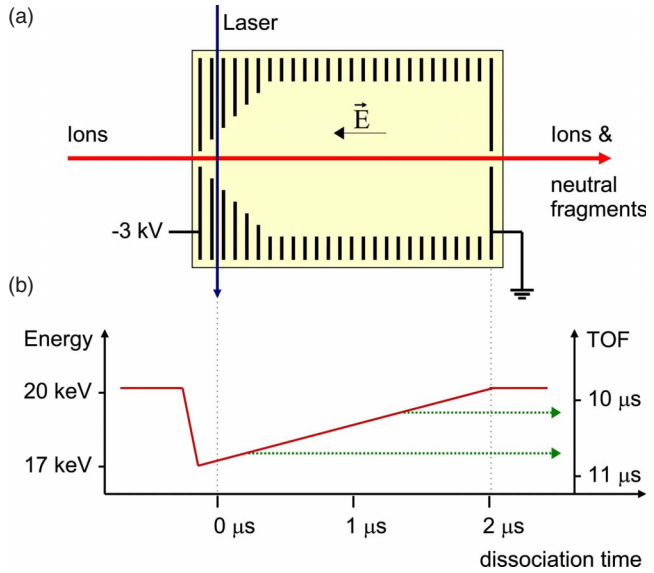

FIG. 4. (Color online) Use of the electric field region to resolve dissociation times (schematically): (a) a stack of electrodes is used for generating a homogeneous electric field; (b) the dissociation time of an ion is mapped to the time of flight (TOF) of its neutral fragments through the varying beam energy over the length of the field region (see text for details).

Through this procedure, the dissociation time of the molecular ions is connected to the TOF of the emerging neutral fragments, which is accessible experimentally. For the pCA^- (pCT^-) chromophore models studied here, dissociation times up to 1.6 (2.0) μs can be resolved, while ions with a dissociation time of 1.6–2.6 (2.0–3.3) μs will fragment in a field-free region after the *E*-field region and thus all exhibit the same TOF. Ions with an even longer dissociation time will reach the deflector before fragmenting and become invisible to the MCP detector.

For interpreting the recorded TOF spectra, a Monte Carlo simulation code is used, which can predict the outcome of an experiment with different assumptions regarding the fragmentation process. In addition to the distribution of dissociation times t_D, another important parameter is the kinetic energy release (KER) of the breakup, since the randomly oriented recoil experienced by the neutral fragments leads to a broadening of the TOF spectra. To disentangle these two contributions, all experiments were repeated with the velocity-changing field turned off. In this situation, the broadening due to kinetic energy release is still visible while the effect of different dissociation times on the TOF is inhibited.

Figure 5 shows some simulated spectra for the pCT^- chromophore. The solid, dotted, and dashed-dotted lines demonstrate the sensitivity of the experiment to different dissociation times, as well as the expected pile-up of slow-fragmentation events at a TOF of 13 μs. While these three curves were obtained for zero recoil, the dashed line shows a simulation assuming a breakup into two fragments of equal mass with a half Gaussian distribution of the kinetic energy release centered at zero and with a width of 200 meV, leading to a symmetrical broadening of the TOF spectrum.

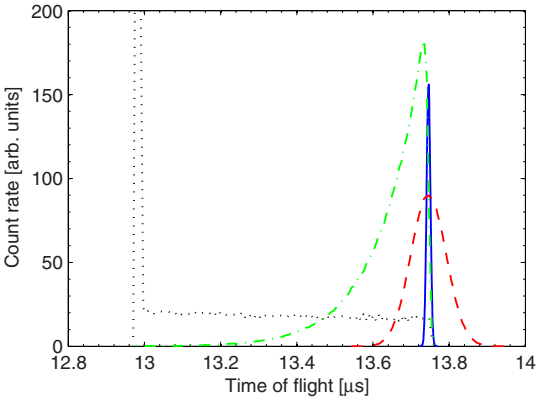

FIG. 5. (Color online) Simulated time-of-flight spectra for neutral photofragments of pCT^-, assuming different distributions of dissociation times t_D: solid line, $t_D=0$; dotted line, random t_D; dashed-dotted line, exponential decay, $\tau=250$ ns; dashed line, $t_D=0$, KER 200 meV.

The fact that the solid curve has a finite width, even though both dissociation time and recoil are set to zero, stems mainly from the finite spatial extension of the laser beam. A smaller (20%) contribution is due to fluctuations in the ion beam energy. The total effect is comparable to that of a fragment kinetic energy release of ~1 meV.

III. RESULTS AND DISCUSSION

A. Merged-beam experiments

The time dependence of the laser-induced fragmentation of pCA^- chromophore anions observed at ELISA is shown in Fig. 6. The signals from both detectors were background substracted and corrected for the time of flight to the detectors. Each data point shown represents the counts originating from one revolution of the ion bunch in the ring. The count rate from the SED was scaled down to 68% to correct for

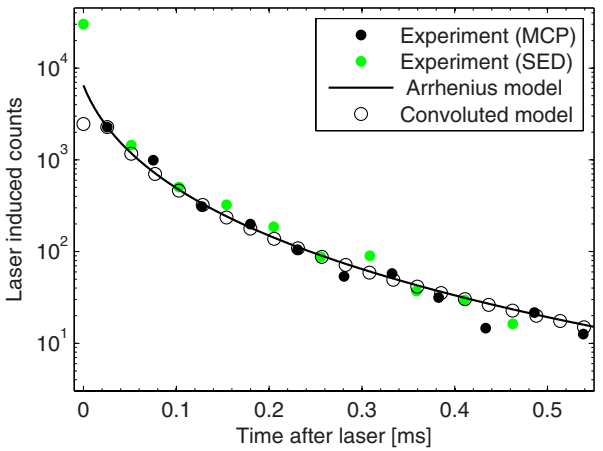

FIG. 6. (Color online) Fragmentation rate of the pCA^- chromophore as measured in ELISA using the MCP and SED detectors (full circles). The solid line was obtained from an Arrhenius-type model calculation, open circles show the signal expected from this model at the given acceptance of the used detectors.

different detection efficiencies of the two detectors.

The experimental data are compared to an over-the-barrier model based on the Arrhenius law

$$k = A \exp\left(-\frac{E_A}{k_B T^*}\right),$$

which is parametrized by the activation energy E_A needed to break the weakest bond of the chromophore molecule, the preexponential factor A, and the emission temperature T^* (see [14,18] for details). With the chosen parameter values (initial ion temperature 300 K, $E_A=2.52$ eV, $A=4.3 \times 10^{17}$ s^{-1}), good agreement with the experiment is found for times larger than 20 μs. The present value for the activation energy compares well with results obtained for other decarboxylation reactions [19]. This suggests that a statistical fragmentation mechanism is indeed responsible for the behavior on long time scales.

The first data point, however, shows a remarkable deviation between the experiment and the model calculation. As shown by the open circles, the count rate expected here when the geometry of the setup is taken into account is well below the pure Arrhenius model value. This is due to the fact that the laser is fired at a time when the ion bunch is located in the center of the ring section visible to the detector, and thus travels through only *half* of this visible region during the time the first data point sums up. For the subsequent revolutions, each data point corresponds to one passage of the ion bunch through the *full* visible region. Compared to this expectation, the experimentally obtained count rate in the first time bin is a factor of 11 higher. Apparently, an additional fragmentation mechanism not covered by the Arrhenius model is active at short (<10 μs) time scales. This fast decay channel is the origin of about 80% of the total fragmentation yield.

For the pCT$^-$ chromophore model, only the first data point from each detector shows a count rate exceeding the residual-gas-induced background rate. This points at a fragmentation process that is either very fast or has a very small cross section. However, at the same time the current of the stored ion beam is found to drop significantly, revealing the removal of ions by a strong photoabsorption process [10]. Thus, the fragmentation in this case is not too rare, but rather too fast to be time resolved at ELISA.

For the daughter ions created in the photofragmentation of pCA$^-$, a mass of 119 ± 2 amu was found, corresponding to the emission of a neutral CO_2 molecule. In the case of pCT$^-$, the observed daughter ion mass is 142 ± 3 amu, which suggests a cleavage of the bond between the thiophenyl group and the main part of the PYP chromophore, with the charge staying at the chromophore side. It should, however, be kept in mind that the technique applied here is not sensitive to the occurrence of very small fragments like hydrogen atoms, or the detachment of an electron.

In the following, we will focus on the fragmentation dynamics on short (microsecond) time scales, which appear to play an important role for both of the molecules under study, and which can be investigated in more detail by time-of-flight measurements in the crossed-beam setup described in Sec. II B.

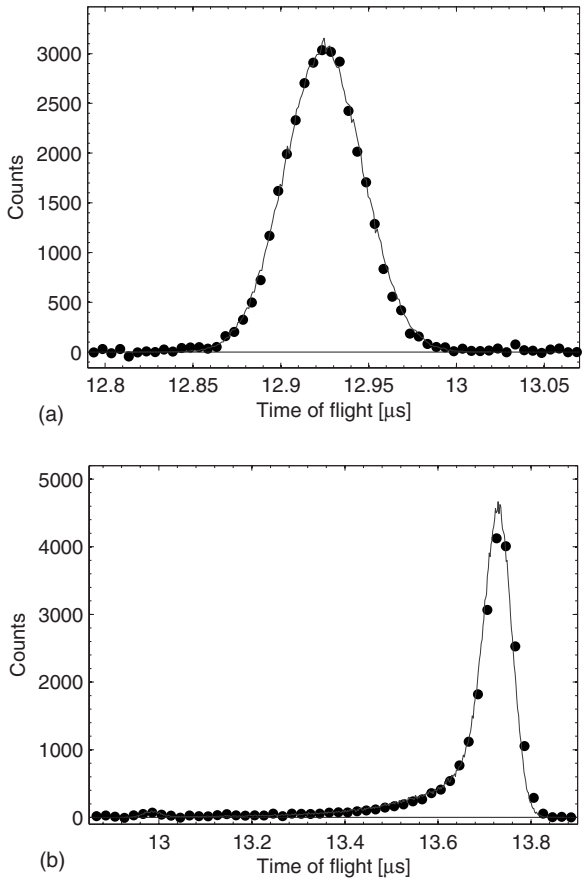

FIG. 7. Time-of-flight spectrum of photoinduced neutral fragments from pCT$^-$ (a) without electric field and (b) with an applied field of 3 kV. Full circles show experimental data taken at a laser wavelength of $\lambda=473$ nm (pulse energy ~ 22 μJ); the solid line is a simulated spectrum (see text for details).

B. Crossed-beam experiments

1. Trans-thiophenyl-p-coumarate

Figure 7 shows the TOF spectrum obtained for photofragmentation of the pCT$^-$ chromophore model in comparison with a simulated data set. As shown in Fig. 7(a), the recoil effect is well described by the simulation when assuming a Gaussian distribution of kinetic energies with a width of $\sigma_E=45$ meV. The time-resolved spectrum taken with the E field [Fig. 7(b)] is in good agreement with a simulation assuming a fast double-exponential decay with time constants $\tau_1=40$ ns (64%) and $\tau_2=300$ ns (34%). For the remaining 2% of fragmentation events, a flat distribution of dissociation times was assumed, corresponding to a slow decay on a $\geqslant 10$ μs time scale.

By varying the laser pulse energy between 2 and 34 μJ, a linear dependence of the count rate on the laser power was found, confirming that the observed fragmentation events stem from a one-photon absorption process.

A more detailed investigation of the actual distributions of dissociation time and kinetic energy release for this molecule is hindered by the fact that both effects have a comparable impact on the observed TOF distribution. However, the combined results of both experiments consistently show that pho-

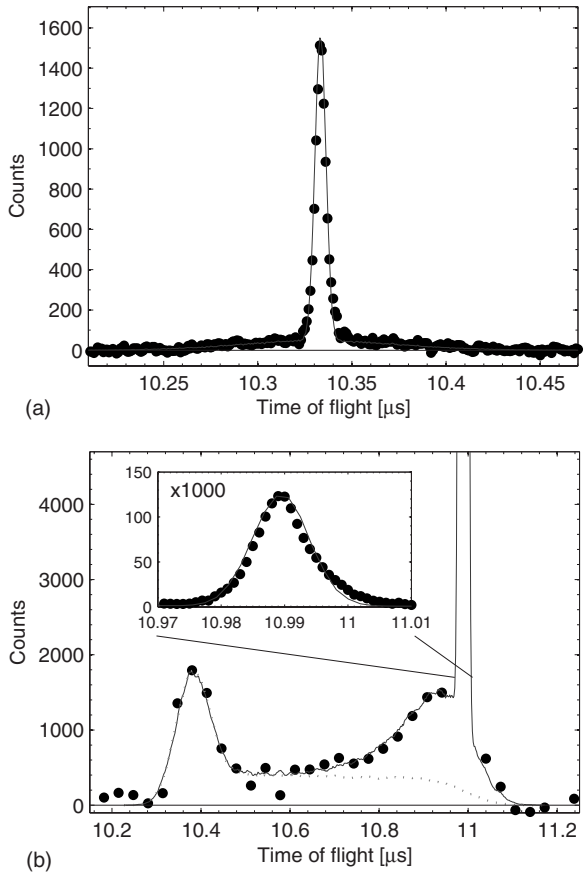

FIG. 8. Time-of-flight spectrum of photoinduced neutral fragments from pCA^- (a) without electric field and (b) with an applied field of 3 kV. Full circles show experimental data taken at a laser wavelength of $\lambda=400$ nm (pulse energy ~ 28 μJ); lines represent simulated spectra (solid line, full simulation; dotted line, Arrhenius-type contribution; see text for details).

toabsorption of the pCT^- chromophore model *in vacuo* predominantly leads to a very fast (100 ns) cleavage of the bond between the chromophore and the thiophenyl group. While other fragmentation processes such as electron detachment cannot be excluded, they are found to yield only minor contributions, if any, to the photoreaction of this molecule. A process involving a very small charged fragment would produce neutrals with near-zero recoil, which would manifest itself in the appearance of a sharp peak in the TOF spectrum (cf. Fig. 5, solid line).

Since the (adiabatic) detachment energy of phenolate lies with 2.25 eV [20] below the photon energy of 2.62 eV applied here, a direct detachment pathway could be expected for this molecule. However, the observed absence of this process suggests that, at the applied photon energy, *vertical* detachment from pCT^- is not possible and that photoexcitation at this energy leads to fragmentation of the molecule rather than delayed electron emission.

2. *Trans-p-coumaric acid*

The corresponding TOF data for the pCA^- model are shown in Fig. 8. Apparently, the fragmentation process is more complex here with both the kinetic energy release and the dissociation time distribution exhibiting two clearly distinguishable components. The time-resolved data in Fig. 8(b) show a two-peak TOF distribution originating from dissociation on the 1 μs time scale (see [17]). A strong additional contribution stemming from very small dissociation times ($\leqslant 2$ ns) results in the sharp peak at a TOF of ~ 11 μs. While the slow contribution shows a significant amount of recoil broadening, the fast peak exhibits no broadening beyond the width caused by the spatial extension of the laser beam. This indicates either a fragmentation with very low KER or the neutralization of the chromophore by electron emission, where essentially all the kinetic energy released is carried away by the electron.

In detail, the simulated data shown in Fig. 8 (solid line) were obtained using the following assumptions: 69% of the observed molecular ions fragment via a fast channel, which is characterized by an exponential decay with $\tau=2$ ns and no recoil. A shorter time constant would also agree with the experiment here, while a longer decay time would manifest itself in an asymmetric broadening of the peak at TOF ~ 11 μs. In terms of recoil, the experimental data support either fragmentation with a KER below 1 meV (assuming the neutral fragment to be CO_2), or electron detachment.

The simulation assumes in addition a slow channel, taken by 31% of the observed ions. Here the KER is modeled by a half Gaussian with $\sigma_E=150$ meV. The dissociation time distribution is once more subdivided into two contributions, an exponential decay with $\tau=200$ ns (12%) plus an Arrhenius-type decay curve (19%), using the same model parameters as for describing the ELISA data on the millisecond time scale. The contribution from Arrhenius-type fragmentation events is indicated by the dotted line in Fig. 8(b). The parameters given here for the slow channel are supported by the experiment within a few percent; deviations of the non-Arrhenius contribution from a purely exponential decay cannot be excluded at the present experimental resolution.

Again, the laser-pulse energy was varied (range 10–190 μJ), yielding a one-photon process as the source of both the slow and the fast decay channels. In addition, the wavelength of the laser light was varied over the width of the absorption peak of the molecule (400–440 nm), and the same branching ratio between the two channels was found over the entire wavelength range.

The most likely interpretation of the data collected for this chromophore model appears to be as follows. By absorbing a photon, the molecule is first brought to an electronically excited, but bound state. A rearrangement of the nuclear geometry then sets in, corresponding to the movement of the original wave packet on the excited potential energy surface (PES). Apparently, two different pathways are open here: one leads to a region where the lowest PES of the neutral molecule comes below the anionic PES supporting the wave packet, thus facilitating autodetachment of an electron. Another pathway leads to a region where a crossing to the anionic ground state PES becomes favorable, resulting in internal conversion of electronic into vibrational energy followed by statistical fragmentation of the molecule.

The assumption of a common starting point for both channels is justified by the observation of a wavelength-independent branching ratio of both channels over the whole

absorption peak. In particular, direct photodetachment of an electron can be excluded, since this would lead to a threshold behavior for the absorption spectrum of the fast channel rather than the observed peak structure. The branching between the two channels and the subsequent electron emission obviously happen on a sub-nanosecond time scale, while the time scale for production of molecular fragments is dominated by the rather slow statistical dissociation from the electronic ground state, which is well described by the Arrhenius model.

The nature of the observed 12% exponential contribution to the slow channel remains an open question. The Arrhenius model does not cover this contribution, even when a higher effective ion source temperature is assumed. A possible explanation thus is a nonthermal distribution of the initial internal ion energies. Such a distribution is indeed expected when extracting ions from a helium-buffered trap, since collisions between the ions and the buffer gas, which lead to internal cooling while the ions are resting in the trap, can cause rovibrational excitation of some molecules at the moment they are accelerated out of the trap. In the storage ring experiments, these excited molecules have time to either dissociate or relax radiatively. However, in the single-pass apparatus the time between extraction from the trap and arrival in the laser interaction region is only a few tens of microseconds. Thus a contribution from collisionally excited ions undergoing much faster statistical dissociation can be expected here.

Another conceivable explanation for the appearance of two fragmentation pathways would be the presence of a mixture of the two isomers of the molecular ion in the experiment, with each isomer fragmenting via one channel only. However, preliminary results obtained for a modified pCA^- chromophore with a well-defined deprotonation site also show fast and slow fragmentation channels [12].

IV. CONCLUSIONS

The absorption dynamics of two PYP chromophore models were studied *in vacuo*. With a velocity-tagging technique that reaches time resolutions down to the nanosecond range, complex dynamics were revealed in the case of the pCA^- model, where at least two channels of very different character (fast electron emission and statistical fragmentation) were found to contribute to the dissociation process. For the pCT^- model, the only photoresponse observed was rather fast fragmentation, which might indicate a statistical process involving a small barrier toward dissociation.

The present results open new possibilities for testing quantum chemical calculations of this benchmark system [21,22], aiming at a detailed understanding of the function of photoactive proteins. On the experimental side, the next step will be to extend the present studies to different chromophore models in order to shed more light on the conditions needed for the appearance of each of the observed fragmentation pathways.

ACKNOWLEDGMENTS

The authors wish to thank Dag Hanstorp for helpful discussions. This work was supported by the Lundbeck Foundation, the Carlsberg Foundation, and the Danish Research Agency (Grant No. 21-03-0330).

[1] S. B. Nielsen, A. Lapierre, J. U. Andersen, U. V. Pedersen, S. Tomita, and L. H. Andersen, Phys. Rev. Lett. **87**, 228102 (2001).
[2] R. Weinkauf, J.-P. Schermann, M. S. de Vries, and K. Kleinermanns, Eur. Phys. J. D **20**, 309 (2002).
[3] I.-R. Lee, W. Lee, and A. H. Zewail, Proc. Natl. Acad. Sci. U.S.A. **103**, 258 (2005).
[4] I. B. Nielsen, L. Lammich, and L. H. Andersen, Phys. Rev. Lett. **96**, 018304 (2006).
[5] S. Brøndsted Nielsen and L. H. Andersen, Biophys. Chem. **124**, 229 (2006).
[6] S. R. Mercier, O. V. Boyarkin, A. Kamariotis, M. Guglielmi, I. Tavernelli, M. Cascella, U. Rothlisberger, and T. R. Rizzo, J. Am. Chem. Soc. **128**, 16938 (2006).
[7] I. B. Nielsen, M. Å. Petersen, L. Lammich, M. B. Nielsen, and L. H. Andersen, J. Phys. Chem. A **110**, 12592 (2006).
[8] L. Lammich, L. H. Andersen, M. Å. Petersen, and M. Brøndsted Nielsen, Biophys. J. **92**, 201 (2007).
[9] R. Y. Tsien, Annu. Rev. Biochem. **67**, 509 (1998).
[10] I. B. Nielsen, S. Boyé-Péronne, M. O. E. Ghazaly, M. B. Kristensen, S. Brøndsted Nielsen, and L. H. Andersen, Biophys. J. **89**, 2597 (2005).
[11] Z. Tian and S. R. Kass, J. Am. Chem. Soc. **130**, 10842 (2008).
[12] J. Rajput *et al.* (unpublished).
[13] J. U. Andersen, P. Hvelplund, S. Brøndsted Nielsen, S. Tomitaa, H. Wahlgreen, S. P. Møller, U. V. Pedersen, J. S. Forster, and T. J. D. Jørgensen, Rev. Sci. Instrum. **73**, 1284 (2002).
[14] L. H. Andersen, H. Bluhme, S. Boye, T. J. D. Jorgensen, H. Krogh, I. B. Nielsen, S. Brøndsted Nielsen, and A. Svendsen, Phys. Chem. Chem. Phys. **6**, 2617 (2004).
[15] D. Hanstorp, Meas. Sci. Technol. **3**, 523 (1992).
[16] K. Støchkel *et al.*, Rev. Sci. Instrum. **79**, 023107 (2008).
[17] L. Lammich, H. Sand, A. Svendsen, I. B. Nielsen, and L. H. Andersen, J. Phys. Chem. A **111**, 4567 (2007).
[18] J. U. Andersen, E. Bonderup, and K. Hansen, J. Chem. Phys. **114**, 6518 (2001).
[19] S. T. Graul and R. S. Squires, J. Am. Chem. Soc. **112**, 2517 (1990).
[20] R. F. Gunion, M. K. Gilles, M. L. Polak, and W. C. Lineberger, Int. J. Mass Spectrom. Ion Process. **117**, 601 (1992).
[21] L. H. Andersen and A. V. Bochenkova, Eur. Phys. J. D (to be published).
[22] E. V. Gromov, I. Burghardt, H. Köppel, and L. S. Cederbaum, J. Am. Chem. Soc. **129**, 6798 (2007).